Geoderma 433 (2023) 116444

Contents lists available at ScienceDirect

Geoderma

journal homepage: www.elsevier.com/locate/geoderma

Nitrogen addition decreases the soil cumulative priming effect and favours soil net carbon gains in *Robinia pseudoacacia* plantation soil

Zhuoxia Su, Zhouping Shangguan *

State Key Laboratory of Soil Erosion and Dryland Farming on the Loess Plateau, Northwest A & F University, Yangling, Shaanxi 712100, China

ARTICLE INFO

Handling Editor: Daniel Said-Pullicino

Keywords:
^{13}C isotope
Priming effect
Microbial phospholipid fatty acids
Microbial life strategy
Soil carbon balance

ABSTRACT

Carbon (C) and nutrient inputs regulate the soil carbon balance by affecting microbial growth and the priming effect (PE). However, we still lack a comprehensive understanding of the microbial mechanism of the soil carbon balance. To examine the regulatory effect of C or nutrient deficiency on microbial C turnover in forest systems of different ages, we collected soil from two *Robinia pseudoacacia* stands of different ages and conducted an incubation experiment using ^{13}C-labelled glucose combined with nitrogen and/or phosphorus (N and/or P) addition. We determined ^{13}C partitioning in CO_2 and phospholipid fatty acids (PLFAs). Glucose and nutrient addition caused both positive and negative PEs during the 30-day incubation. The PE of the 15-year-old (15Y) stand changed from positive (0–15 days) to negative (15–30 days), while the PE of the 45-year-old (45Y) stand ranged from negative (0.5 days) to positive (after 1 day). Different microbial mechanisms play diverse roles during various decomposition stages. The 45Y stand led to a higher cumulative positive PE than the 15Y stand. For both stands, fungi assimilated a greater proportion of ^{13}C-glucose in the glucose plus nitrogen (CN addition) treatment than in the glucose addition alone treatment, which alleviated the fungal N requirements and decreased the cumulative PE. However, the glucose plus phosphorous treatment (CP addition) had no significant influence on the cumulative PE. CN addition favoured high-yielding microbial strategists (Y-strategists) and glucose-derived SOC accumulation. This phenomenon was supported by the relatively high microbial carbon use efficiency (CUE), which increased the soil net C balance. In contrast, CP addition was conducive to resource-acquisition strategists (A-strategists), which increased soil organic carbon mineralization and decreased the soil net C balance. This was evidenced by higher ^{13}C incorporation into the PLFAs of gram-positive bacteria and the positive PE for C and nutrient acquisition under CP addition. Consequently, CN addition decreased the cumulative PE and increased ^{13}C-fungi and CUE, which favoured the soil net C gain. Our study highlights the importance of N fertilization for soil C sequestration in *Robinia pseudoacacia* plantations.

1. Introduction

Soil is the largest carbon pool in terrestrial ecosystems, and the stabilization of soil carbon depends on the balance of the input of plant-derived carbon and the loss through soil mineralization (Jackson et al., 2017; Scharlemann et al., 2014). As an important component of terrestrial ecosystems, the carbon stocks of forest ecosystems account for 70% of the global carbon pool (Chen et al., 2019; Jandl et al., 2007). When labile organic matter enters the soil, it affects soil organic matter (SOM) decomposition and results in increasing or decreasing soil organic carbon (SOC) output, which is called the priming effect (PE) (Blagodatskaya and Kuzyakov, 2008; Kuzyakov et al., 2000). *Robinia pseudoacacia* is a main afforestation tree species on the Loess Plateau of China, and vegetation restoration has influenced plant productivity, community composition and litter biomass (Zhang et al., 2019; Zhong et al., 2020); therefore, it may change the input of plant-derived carbon into the soil. However, the amount of soil carbon loss caused by plant-derived carbon during vegetation restoration is still unclear. Consequently, it is important to understand the regulating mechanisms impacting the PE in afforestation areas on the Loess Plateau of China.

The priming effect is a process involving the interaction of many factors and mechanisms (Kuzyakov, 2010). Many factors affect the priming effect, such as the soil SOC content, pH, and nutrient addition (Mo et al., 2022; Ren et al., 2022; Sun et al., 2019). Nutrient availability has been considered the main factor regulating the priming effect among these variables (Feng and Zhu, 2021). At present, two mechanisms have

* Corresponding author at: Xinong Rd. 26, Institute of Soil and Water Conservation, Yangling, Shaanxi 712100, China.
E-mail address: shangguan@ms.iswc.ac.cn (Z. Shangguan).

https://doi.org/10.1016/j.geoderma.2023.116444
Received 13 September 2022; Received in revised form 13 March 2023; Accepted 20 March 2023
Available online 28 March 2023

Table 1
The basic physicochemical characteristics of the soil from the two stands.

Soil	Location	pH	Total C (g kg^{-1})	Total N (g kg^{-1})	Total P (g kg^{-1})	Soil moisture (%)	δ ^{13}C ‰
15 years (15Y)	108°5′6″E, 34°50′39″N	7.97 ± 0.02	10.15 ± 0.13	1.13 ± 0.02	0.71 ± 0.00	21.99 ± 0.44	–23.69 ± 0.49
45 years (45Y)	108°5′9″E, 34°50′20″N	6.68 ± 0.03	13.96 ± 0.37	1.53 ± 0.08	0.54 ± 0.01	29.73 ± 2.15	−26.26 ± 0.07

Data presented are the means ± standard deviations (SD).

been proposed to explain the priming effect, but the particular mechanism is influenced by substrate stoichiometry and microbial demand for nutrients (Craine et al., 2007). 'Microbial stoichiometric decomposition' theory indicates that when substrate stoichiometry matches microbial demand, fast-growing microbes (r-strategy) stimulate microbial decomposition by increasing microbial activities and then lead to a positive priming effect (Zhang et al., 2020; Zhang et al., 2021). 'Microbial N mining' theory suggests that microorganisms use labile carbon as energy to decompose SOM for N acquisition (Blagodatskaya and Kuzyakov, 2008; Chen et al., 2014). Previous studies have paid more attention to the effect of N addition on PE (Li et al., 2018; Liao et al., 2020; Zhang et al., 2021; Zheng et al., 2022), with a few studies investigating the effect of P addition on the priming effect, but this remains an open question. A study reported that P or NP addition had no significant influence on the priming effect in subtropical soil (Feng et al., 2021). Li et al. (2020) showed that P addition significantly increased the priming effect on the Tibetan Plateau. Microbial P limitation increased with increasing stand age of *Robinia pseudoacacia* (Zhang et al., 2019; Zhong et al., 2020), which indicates that the microbial demand for P changes. Hence, we need to focus on the role of P and NP addition in mediating the priming effect and explore the related mechanism.

Carbon and nutrient availability may influence different microbial functional groups and mediate the priming effect and soil carbon balance (Hicks et al., 2019; Zhu et al., 2022). First, carbon substrate availability may affect the succession of copiotrophs and oligotrophic microorganisms. R-strategists use labile glucose to grow quickly at the beginning; when glucose is exhausted, K-strategists have more advantages in using recalcitrant organic matter (Cui et al., 2020; Deng et al., 2020; Fu et al., 2022). A previous study linked 'microbial N mining' theory to the k-strategy and 'stoichiometry decomposition' theory to the r-strategy (Chen et al., 2014). In addition, nutrient availability may affect the relative abundance of microbial functional groups (Fontaine et al., 2011). Previous studies have demonstrated that nitrogen addition affects the relative abundance of fungi (Fanin et al., 2014; Liu et al., 2013), while P addition influences bacterial growth (Nottingham et al., 2017). Understanding the role of different microbial groups under N and P addition has critical significance for the soil carbon balance. A framework of microbial life strategies was developed to predict the interactions of microbial growth with their resources, as these processes largely influence the soil carbon cycle and balance (Malik et al., 2019a). The absence of resource limitation and stress favours the high-yield strategy (Y-strategy), while microorganisms will choose to increase resource acquisition at the expense of growth under low-resource availability (A-strategy) (Malik et al., 2019a; Malik et al., 2019b; Shao et al., 2021). However, the effect of microbial life strategies on the soil carbon balance under N and P addition is still unclear.

Here, we sampled soil from different stand ages of *Robinia pseudoacacia* during vegetation restoration and conducted a 30-day incubation experiment combined with ^{13}C-glucose and nutrient (N and/or P) additions. We measured different sources of CO_2 and associated soil properties, mainly including soil nutrient availability, extracellular enzyme activities and ^{13}C-PLFAs. We aimed to (1) study the effect of carbon and nutrient input on the temporal dynamics of PE and the related mechanism; (2) elucidate the effect of carbon and nutrient addition (N and/or P) on the cumulative PE and soil carbon balance and explore how soil microbial traits regulate PE and the net soil carbon balance; and (3) investigate how stand age affects the cumulative priming effect. We hypothesized that (1) the PE intensity decreases with incubation duration. It may be that the input of labile carbon in the early stages stimulates microbial activity, leading to stronger SOC mineralization. (2) Glucose combined with nutrient addition leads to a lower PE when compared with glucose addition alone. Nutrient addition alleviates microbial demand and decreases microbial N mining, which favours soil net C gains. (3) Older stands have a higher SOC content and lower cumulative PE than younger stands.

2. Materials and methods

2.1. Study sites and soil characterization

Soil was collected from two *Robinia pseudoacacia* stands (15 years and 45 years) in the Huaiping forest in Yongshou County, Shaanxi Province, southern Loess Plateau of China (34°50′N, 108°5′E). The *Robinia pseudoacacia* plantations were located 1377.6–1379.5 m above sea level. The annual temperature is 10.8 °C, with a mean minimum temperature of − 2.9 °C in January and a mean maximum temperature of 23.7 °C in July (Liu et al., 2020). The annual precipitation is 605 mm; this area is characterized by a subhumid climate region. The soil is classified as loess (Calcaric Regosol in the WRB soil classification) (Liu et al., 2022). The physicochemical characteristics of the soils are given in Table 1. Soil samples were collected from the top layer (0–20 cm) in August 2020. After removal of the plant residues, roots, and visible stones, the soil samples were homogenized and sieved (2 mm). Fresh soil was transported to the laboratory on dry ice; one part was stored at 4 °C for the incubation experiment, and the other part was air-dried to analyse the soil physical and chemical properties.

2.2. Experimental design and laboratory incubation

Fresh soil samples were weighed (25 g dry weight) into 250 mL sealable jars and adjusted to 60% field water capacity by the addition of deionized water. Each bottle had a rubber stopper, which was fitted with two glass tubes and two-way valves. All samples were preincubated for 2 weeks at 25 °C. A single dose of ^{13}C-labelled glucose was added. The glucose consisted of a 1:20 mixture of ^{13}C-labelled glucose (uniformly labelled, U-$^{13}C_6$, > 99 atom%, Cambridge Isotope Laboratories, Andover, MA, USA) and non-labelled glucose. The final solution was diluted to a final ^{13}C abundance containing 5.15 atom % ^{13}C (δ ^{13}C value of 3856‰).

After preincubation, the following treatments were applied to the soil samples: "control with deionized water" for the CK treatment, "^{13}C-labelled glucose" for C addition, "^{13}C-labelled glucose plus N" for CN addition, "^{13}C-labelled glucose plus P" for CP addition, and "^{13}C-labelled glucose plus N and P combined" for CNP addition ("CK", "C", "CN", "CP", and "CNP", respectively). Carbon substrate was added at the rate of 2% average SOC content, according to a similar rate with a range of 1–2% of the initial soil organic C (Feng et al., 2021; Wu et al., 2020; Zhao et al., 2022). The average SOC content of the soil from the two stands was 12.06 g C kg^{-1} soil, and the carbon addition rate was 0.2411 mg C g^{-1} soil. The rate of nitrogen addition was 0.05 mg N g^{-1} soil as

ammonium chloride (NH_4Cl), and the phosphorus addition rate was 0.05 mg P g^{-1} soil as potassium dihydrogen phosphate (KH_2PO_4). The amounts of N and P addition were based on two aspects. First, previous studies reported that the N addition rate for forest ecosystems on the Loess Plateau was 0–12 g N m^{-2} y^{-1}, which changed the soil N content from a limited state to a saturated state (Jing et al., 2021). Increasing studies have shown that microorganisms are limited by nutrients during the process of vegetation restoration and that the supply of soil nutrients affects microorganism metabolism. Therefore, we chose an adequate supply of nutrients (12 g N m^{-2} y^{-1}) to avoid nutrient limitation. Mineral N was applied at a rate of 0.05 mg N g^{-1} soil equivalent to approximately 12 g N m^{-2} y^{-1} to a depth of 20 cm (bulk density of 1.25 g cm^{-3}). Additionally, we referenced N and P levels selected in PE experiments on the Loess Plateau or in forest studies (Cui et al. 2022; Feng et al. 2021). The element addition amount, soil nutrient content and soil stoichiometry are shown in the supplementary information (Table S1). Carbon, CN, CP, and CNP were applied in the form of a 2 mL solution. Deionized water (2 mL) was added to the unamended control soils. All solutions were added to the soil surfaces in a drip-by-drop rotation to ensure homogeneity. Soil samples were incubated at 25 °C for 30 days. A total of 120 jars were sealed with rubber plugs, among which 30 jars were fixed to collect gas and 90 jars were used to collect soil (2 stand ages × 5 treatments × 3 soil sampling events × 3 replicates). We added deionized water to maintain a 60% field water content for microbial growth in the incubation process.

The mineralization of added glucose and native SOC was quantified according to CO_2 production. Gas samples were taken from the jars for total CO_2 and δ ^{13}C analyses at 0.5, 1, 3, 5, 7, 10, 15, 20, and 30 days after incubation. To ensure that there was no CO_2 in the jar at the beginning of the CO_2 flux measurement, we removed the jars from the incubator prior to gas collection, and then high-purity CO_2-free air was used to flush the jar headspace for approximately 1 min to standardize the initial CO_2 concentration (Zhang et al., 2021). Next, the two two-way valves were closed to seal the jar. Subsequently, the jar was returned to the incubator, and gas was collected at 0 and 2 h. Two CO_2 samples were taken per replicate during each sampling event. One gas sample was collected in a 30 mL syringe, which was used to measure the total CO_2 concentration using a GC-9790II gas chromatograph. Another CO_2 sample was injected into a 12 mL round-bottom vacuum flask, and the gaseous atom% abundance values were determined by isotope ratio mass spectrometry. After gas sampling, the jars were exchanged with the atmosphere for 0.5 h. Meanwhile, other samples used for soil collection were also taken out of the incubator and exchanged with air for 0.5 h. Soil samples were destructively collected on days 1, 15, and 30 and used to analyse soil available nutrients (SAP, NH_4^+-N, DOC), enzyme activities (BG, CBH, NAG, AP) and phospholipid fatty acids (PLFAs).

2.3. Laboratory analyses

2.3.1. Soil property analyses

The soil organic carbon was oxidized by potassium dichromate. The soil total nitrogen content was measured by the Kjeldahl method. Soil total phosphorus was measured by the $HClO_4$-H_2SO_4 method (Bao, 2000). Soil pH was measured by a pH meter with a soil to water ratio of 1:2.5 (w/v). Soil moisture was measured by drying the soil in a 105 °C oven for 8 h. Dissolved organic carbon (DOC) was extracted with 0.5 M K_2SO_4 and then measured by a TOC analyser (Liauid TOC II, Elementar, Germany). Soil available phosphorus (SAP) was extracted with 0.5 M $NaHCO_3$ and then measured via an ultraviolet spectrophotometer (Hitachi UV2300). Soil ammonium N (NH_4^+-N) was extracted from the soils with 1 M KCl and analysed by a continuous flow analyser (Auto-analyzer 3, Bran and Luebbe, Germany). The soil C isotope ($\delta^{13}C$) was measured by an isotope ratio mass spectrometer (IR-MS) (MAT 253; Thermo Scientific, Waltham, MA, USA).

2.3.2. Soil extracellular enzyme activities

The activities of four soil extracellular enzymes were measured, i.e., carbon decomposition enzymes (BG: β-1,4-glucosidase; CBH: cellobiohydrolase), nitrogen decomposition enzyme (NAG: β-1,4-N-acetyl-glucosaminidase) and phosphorus decomposition enzyme (AP: phosphatase). All potential enzyme activities were measured in 96-well microplates. Enzyme assays were performed by following the methods of DeForest (2009) and Saiya-Cork et al. (2002) with some modifications. Specifically, one gram of soil was mixed with 50 mL of buffer to form a sample suspension. Samples, enzyme substrates, reference standards and buffer were placed in specific wells in the plate. The standard substance for BG, CBH, NAG, and AP was 4-methylumbelliferone, and the substrates were 4-MUB-β-D-glucopyranoside, 4-MUB-cellobioside, 4-MUB-N-acetyl-β-D-glucosaminide, and 4-MUB-phosphate. Their incubation times were 2 h, 4 h, 4 h and 0.5 h, respectively. The reaction was stopped by NaOH solution, and the fluorescence was measured with excitation at 365 nm and emission at 450 nm (Spectra Max M2, Molecular Devices, California, USA). The unit of enzyme activity was nmol h^{-1} g^{-1}.

2.3.3. Phospholipid fatty acid (PLFA) extraction and analysis

On days 1, 15 and 30, the soil microbial PLFAs were extracted, fractionated, and purified according to the methods described by Yuan et al. (2016). In short, approximately 2 g freeze-dried soil was extracted twice using a solution of citrate buffer: chloroform: methanol (0.8:1:2 v/v/v) and then centrifuged for 10 min. Then, phospholipids were separated from neutral lipids and glycolipids via a silica acid column (Supelco, Bellefonte, PA, USA). After mild alkaline methanolysis, phospholipids were methylated to their fatty acid methyl esters (FAMEs). A gas chromatograph (N6890; Agilent, Santa Clara, CA, USA) equipped with a MIDI Sherlock microbial identification system (Version 4.5; MIDI, Newark, DE, USA) was used to separate and identify FAMEs. The internal standard of methyl nonadecanoate fatty acid (19:0) was used to quantify the phospholipid concentrations. A Trace GC Ultra gas chromatograph (GC) with a combustion column attached via GC Combustion III to a Delta V Advantage isotope ratio mass spectrometer (IRMS; Thermo Finnigan, Germany) was used to analyse the δ ^{13}C of each PLFA. The following PLFAs were used as markers for bacteria: i15:0, a15:0, i16:0, and i17:0 for gram-positive bacteria (G^+) and 16:1ω7c for gram-negative bacteria (G^-); 18:1ω9c and 18:2w6c were used as biomarkers for fungi (F), and 10Me16:0 PLFAs were used as biomarkers for actinomycetes (A). Nonspecific (universal) PLFAs were represented by 16:0 and 18:0.

2.4. Calculations

2.4.1. Total CO_2 emissions

The ^{13}C atom-% of enriched sample CO_2 was determined using an isotope ratio mass spectrometer (MAT 253; Thermo Scientific, Waltham, MA, USA) coupled with a gas bench system (Thermo Scientific, Waltham, MA, USA) at the Institute of Subtropical Agriculture, Chinese Academy of Science. The emission flux of CO_2 was calculated according to Eq. (1) and (2). The actual air temperature was used to correct all CO_2 efflux rates (Van Zwieten et al., 2010).

$$A = \frac{\Delta c}{\Delta t} \times \frac{M \times V}{m \times MV_{corr}} \quad (1)$$

where A is the CO_2-C efflux (mg C kg^{-1} soil h^{-1}); $\frac{\Delta c}{\Delta t}$ is the change in the CO_2 content per unit time (ppm h^{-1}); M is 12 g mol^{-1} of molecular weight of carbon; V is the effective volume at the top of the jars (L); m is the soil dry weight (g); and MV_{corr} is the molecular volume (L mol^{-1}), which needs to be corrected based on the following equation (2):

$$MV_{corr} = 22.4 \times \frac{273.15 + T}{273.15} \quad (2)$$

where T is the incubation temperature, 22.4 (L) is the molar volume of an ideal gas at 1 atm and 273.15 K (Zhang et al., 2021)

The cumulative CO_2 emissions were calculated as follows:

$$Z = \sum \frac{A_{i-1} + A_i}{2} \times (t_{i-1} - t_i) \times 24 \quad (3)$$

where Z represents the cumulative CO_2 emissions (mg C kg^{-1} soil); A_{i-1} and A_i are the CO_2 gas emission fluxes at the i th and $(i-1)$th sampling times, respectively; and $(t_{i-1} - t_i)$ is the interval time between the i th and $(i-1)$th collecting gas (day, 24 h).

2.4.2. Partitioning of CO_2 sources and quantifying PE and net C balance

We use a two-pool isotope-mixing model to calculate the glucose-derived CO_2 ($CO_{2glucose}$) and SOM-derived CO_2 (CO_{2SOM}):

$$CO_2 glucose = CO_2 total \times \frac{atom\%^{13}CO_{2SOM} - atom\%^{13}CO_{2total}}{atom\%^{13}CO_{2SOM} - atom\%^{13}CO_{2glucose}} \quad (4)$$

where $CO_{2glucose}$ is the glucose-derived CO_2, CO_{2total} represents the CO_2 from glucose-amended soil; $atom\%^{13}CO_{2SOM}$ is the ^{13}C atom-% value of the CO_2 derived from glucose-unamended soil; $atom\%^{13}CO_{2total}$ is the ^{13}C atom-% value of the CO_2 derived from glucose-amended soils; and $atom\%^{13}CO_{2_{glucose}}$ is the ^{13}C atom-% value of the labelled glucose (5.15 atom%).

$$CO_{2SOM} = CO_{2total} - CO_{2glucose} \quad (5)$$

CO_{2SOM} is the SOM-derived CO_2, and CO_{2total} represents the CO_2 from glucose-amended soil.

$$PE(\text{Priming effect}) = CO_{2SOM} - CO_{2CK} \quad (6)$$

CO_{2CK} refers to the basal respiration (from the control (unamended) treatment).

$$\text{Relative PE}\,(\%) = \frac{\text{amended}\,CO_{2\,SOM-derived} - \text{unamended}\,CO_{2_{CK}}}{\text{unamended}\,CO_{2_{CK}}} \times 100 \quad (7)$$

where amended $CO_{2SOM\text{-}derived}$ and unamended CO_{2CK} are the cumulative CO_2 emissions (mg C g^{-1} soil) from SOM in the glucose-amended soil and from control (unamended) soil, respectively.

The net soil C balance at the end of incubation was calculated as the difference between glucose-derived SOC and the carbon loss due to the PE (Wu et al., 2020; Zhu et al., 2022). "Glucose-derived SOC" means the glucose-derived C remaining in soil (^{13}C remaining in soil), which can be calculated as the difference between the amount of added glucose (^{13}C added) and cumulative glucose-derived CO_2 (^{13}C lost as CO_2) (Fontaine et al., 2004; Zhu et al., 2022).

2.4.3. ^{13}C-PLFA calculation

Glucose-derived C in individual PLFAs (P_i; μg C g^{-1} soil) was calculated using the following equation:

$$P_i = C_i \times (atom\%^{13}C - PLFA_{Total} - atom\%^{13}C - PLFA_{ck}) / (atom\%^{13}C_{glucose} - atom\%^{13}C - CPLFA_{ck}) \quad (8)$$

where C_i is the C content (μg C g^{-1} soil) of the individual PLFAs. Atom% ^{13}C-PLFA $_{Total}$ and $atom\%^{13}C$-$PLFA_{CK}$ represent the ^{13}C atom-% values of each PLFA in soil with or without glucose addition. $^{13}C_{glucose}$ is the ^{13}C atom-% value of the labelled glucose.

Total substrate-derived C in the gram-positive bacteria (G^+), gram-negative bacteria (G^-), actinomycete (A), fungal (F) and bacterial (B) groups (P_t; ug C g^{-1} soil) was quantified according to the following equation:

$$P_t = \sum P_i \quad (9)$$

The total PLFA content was calculated as the sum of G^+, G^-, A, F and unspecified PLFAs. The microbial carbon efficiency was calculated as glucose-derived C incorporated into PLFAs relative to its total consumption (glucose-derived C into PLFAs + glucose-derived C respired) (Hicks et al., 2019). In addition, we quantified the turnover rate (% day^{-1}) of PLFAs at each sampling time according to Deng et al. (2020).

2.4.4. Calculation of microbial C and nutrient limitation

Microbial C limitation (vector length) and microbial nutrient limitation (vector angle) were calculated based on the ratio of untransformed activities for all data (Li et al., 2022). The vector length represents the relative C limitation, and the vector angle quantifies the relative P versus N acquisition (Fanin et al., 2016). The vector length is calculated as follows:

$$Vector\ length = SQRT\left(x^2 + y^2\right) \quad (10)$$

The vector angle is expressed as follows:

$$Vector\ angle\ (^\circ) = DEGREES(ATAN2(x,\ y)) \quad (11)$$

where x represents [(BG + CBH)]/[BG + CBH + AP] for the relative activity of C- versus P-enzymes, and y is [(BG + CBH)]/[BG + CBH + NAG] for the relative activity of C- versus N-enzymes (Moorhead et al., 2016). The relative C limitation increased with vector length. A vector angle $> 45^\circ$ represents relative P limitation, whereas a vector angle $< 45^\circ$ indicates relative N limitation.

2.5. Data analysis

Three-way ANOVA was used to assess the effects of nutrient addition, stand age and incubation time on soil available C:N:P stoichiometry, enzyme C:N:P stoichiometry, microbial metabolic limitations, ^{13}C-PLFAs, CUE and microbial turnover rate. At the end of the incubation (30 days), we used two-way ANOVA to examine the effect of stand age and nutrient treatment on total CO_2, glucose-derived CO_2, soil-derived CO_2, the priming effect and net C balance. The difference in different nutrient additions at each sampling time was evaluated using one-way ANOVA. Differences were considered significant at $P < 0.05$ followed by Duncan's test. All of the above statistical analyses were performed with IBM SPSS version 20.0, and the bar graph was generated using Origin 2018 (OriginLab Corporation, Northampton, MA, USA).

Pearson's test was used to determine correlations among soil available C:N:P stoichiometry, enzyme C:N:P stoichiometry, microbial metabolic limitations, ^{13}C-PLFAs, CUE and soil cumulative PE. Structural equation modelling (SEM) was conducted using AMOS software version 24.0. SEM was used to explore direct and indirect relationships among the soil cumulative PE, nutrient addition, soil available C:N:P stoichiometry, enzyme C:N:P stoichiometry, ^{13}C-PLFA and $^{13}CO_2$ efflux. Principal component analysis was conducted to create a multivariate functional index prior to SEM analysis. The variables DOC/NH_4^+-N, DOC/SAP and NH_4^+-N/SAP were used to create a multivariate functional index to represent soil available C:N:P stoichiometry. The variables (BG + CBH):NAG, (BG + CBH):AP, and NAG:AP were used to generate a functional index representing enzyme C:N:P stoichiometry. The ^{13}C-G^+, ^{13}C-G^-, ^{13}C-fungi and ^{13}C-bacteria were used to generate a functional index representing microorganisms. The first component (PC1) explained 43–76% of the total variance, and then we introduced it as a new variable into the SEM analysis. The model with the best fit was derived by using maximum likelihood with the model fit determined with the use of the chi-squared test ($\chi 2$), p values, goodness-of-fit index (GFI), root mean square errors of approximation (RMSEA), and standard root mean-square residual (SRMR). The model fit was improved iteratively by removing or adding relationships between the observed variables (nodes) in prior models according to a number of modification indices.

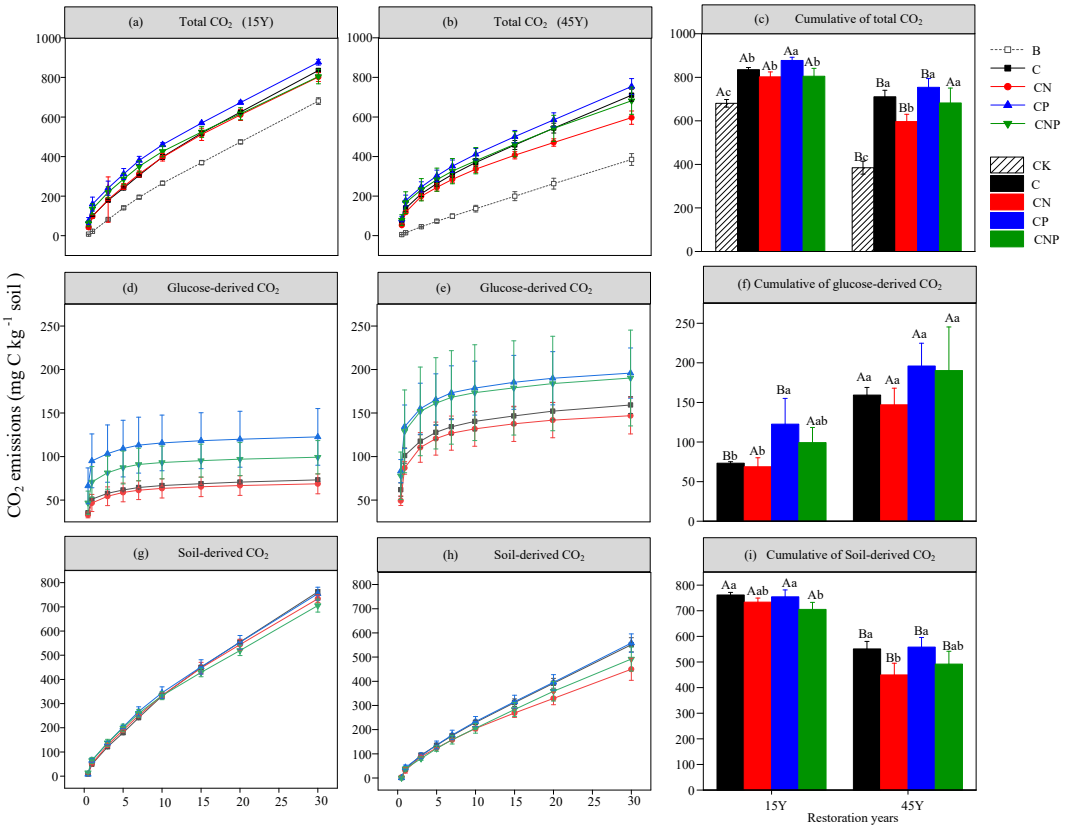

Fig. 1. Trends of cumulative CO_2 efflux (mg CO_2-C kg^{-1} soil) from total CO_2, glucose-derived CO_2, SOM-derived CO_2, and the priming effect. The first column (a, d, and g) represents the 15-year-old stand. The second column (b, e, and h) represents the 45-year-old stand. The bar plot shows the data of all treatments at the end of the 30-day incubation. Values are presented as the mean ± standard deviation (SD) (n = 3). C: glucose addition, CN: glucose plus N addition, CP: glucose plus P addition, CNP: glucose plus NP addition. Values followed by different lowercase letters indicate significant differences among the nutrient addition treatments within a restoration age, and values followed by different uppercase letters indicate significant differences at different restoration ages under the same nutrient treatment. Significance levels were set at $P < 0.05$.

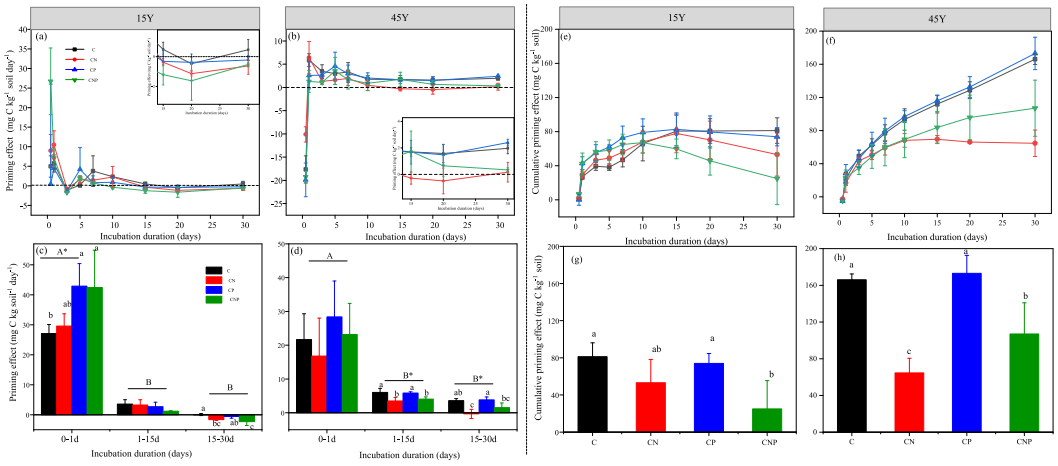

Fig. 2. The left panel represents the priming effect of glucose and nutrient additions on native soil organic C mineralization over the entire 30-day incubation (a and b) and during three sampling periods (c and d). The right panel represents the cumulative priming effect over the entire 30-day incubation (e and f) and cumulative priming effect values at the end of 30 days (g and h) among different treatments. Values are presented as the mean ± SD (n = 3). C: glucose addition, CN: glucose plus N addition, CP: glucose plus P addition, CNP: glucose plus NP addition. Different capital letters displayed at the top of the bars (c and d) represent significant differences between periods. Asterisks (c and d) indicate significant differences between treatments within a period. Different lowercase letters above the bars represent significant differences among treatments within a period. Significance levels were set at $P < 0.05$.

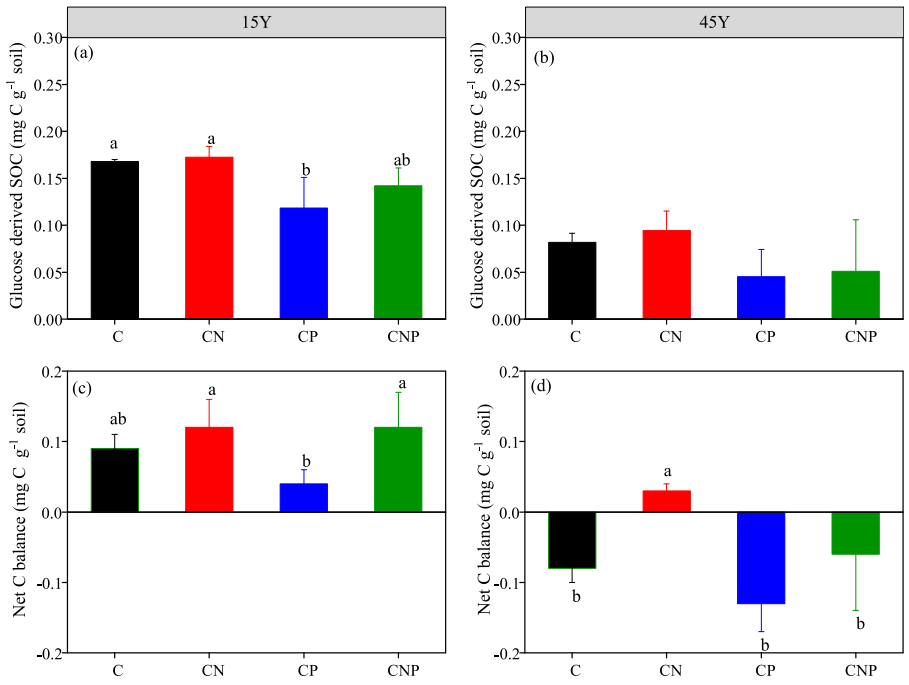

Fig. 3. Glucose-derived SOC and net soil C balance under different nutrient plus glucose treatments after 30 days of incubation. Values represent means ± standard deviations (n = 3). Lowercase letters indicate significant differences ($P < 0.05$) among different nutrient treatments.

3. Results

3.1. Total CO_2, glucose-derived CO_2, and soil-derived CO_2 emission dynamics

The total cumulative soil CO_2 was significantly influenced by stand age, nutrient treatment and their interaction ($P < 0.01$, Table S2). The total cumulative soil CO_2 emission amounted to 350.51–885.75 mg C kg^{-1} soil at the end of incubation across all treatment combinations (Fig. 1 a-c). Total CO_2 emissions were significantly higher in the 15Y stand than in the 45Y stand. In terms of nutrient treatment, the application of glucose in combination with N (CN) decreased total CO_2 efflux by 3.92% and 16.01% compared with glucose addition alone in the 15Y stand (Fig. 1c, $P > 0.05$) and 45Y stand ($P < 0.05$). Moreover, stand age and nutrient treatment significantly influenced glucose-derived CO_2 and soil-derived CO_2 emissions. Compared with glucose addition alone, additional N and NP application decreased soil-derived CO_2 emissions in both stands (Fig. 1 g-i).

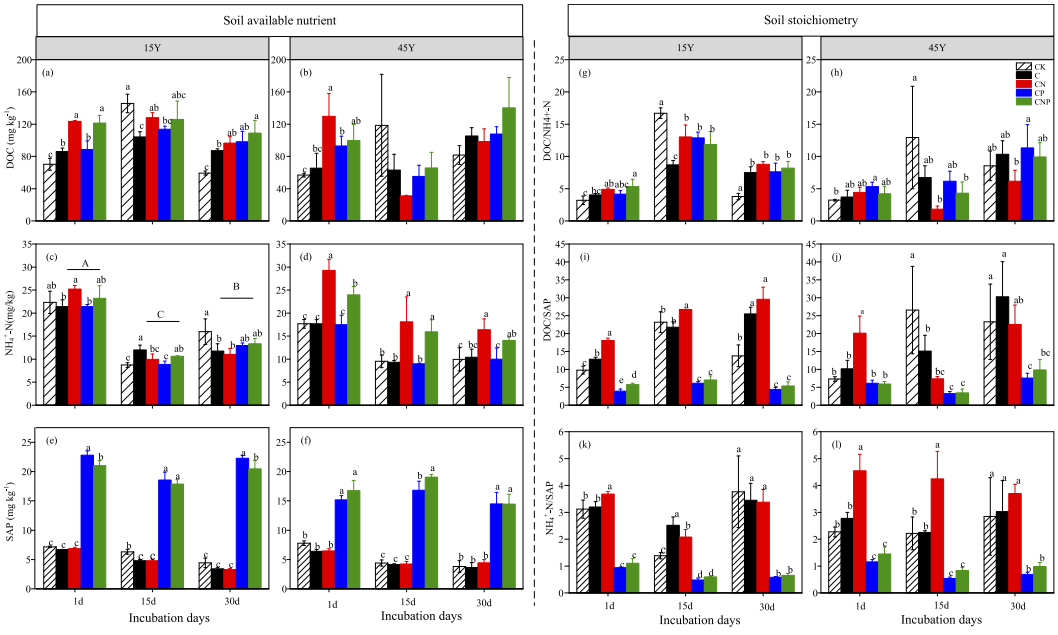

Fig. 4. Changes in soil available nutrients and ratios after 1, 15, and 30 days of glucose and nutrient addition. Values represent means ± SDs (n = 3). DOC: dissolved organic carbon; NH_4^+-N: ammoniacal nitrogen; SAP: soil available phosphorus; DOC/NH_4^+-N: DOC to NH_4^+-N ratio; DOC/SAP: DOC to SAP ratio; NH_4^+-N/SAP: NH_4^+-N to SAP ratio. Lowercase letters indicate significant differences ($P < 0.05$) among different nutrient treatments.

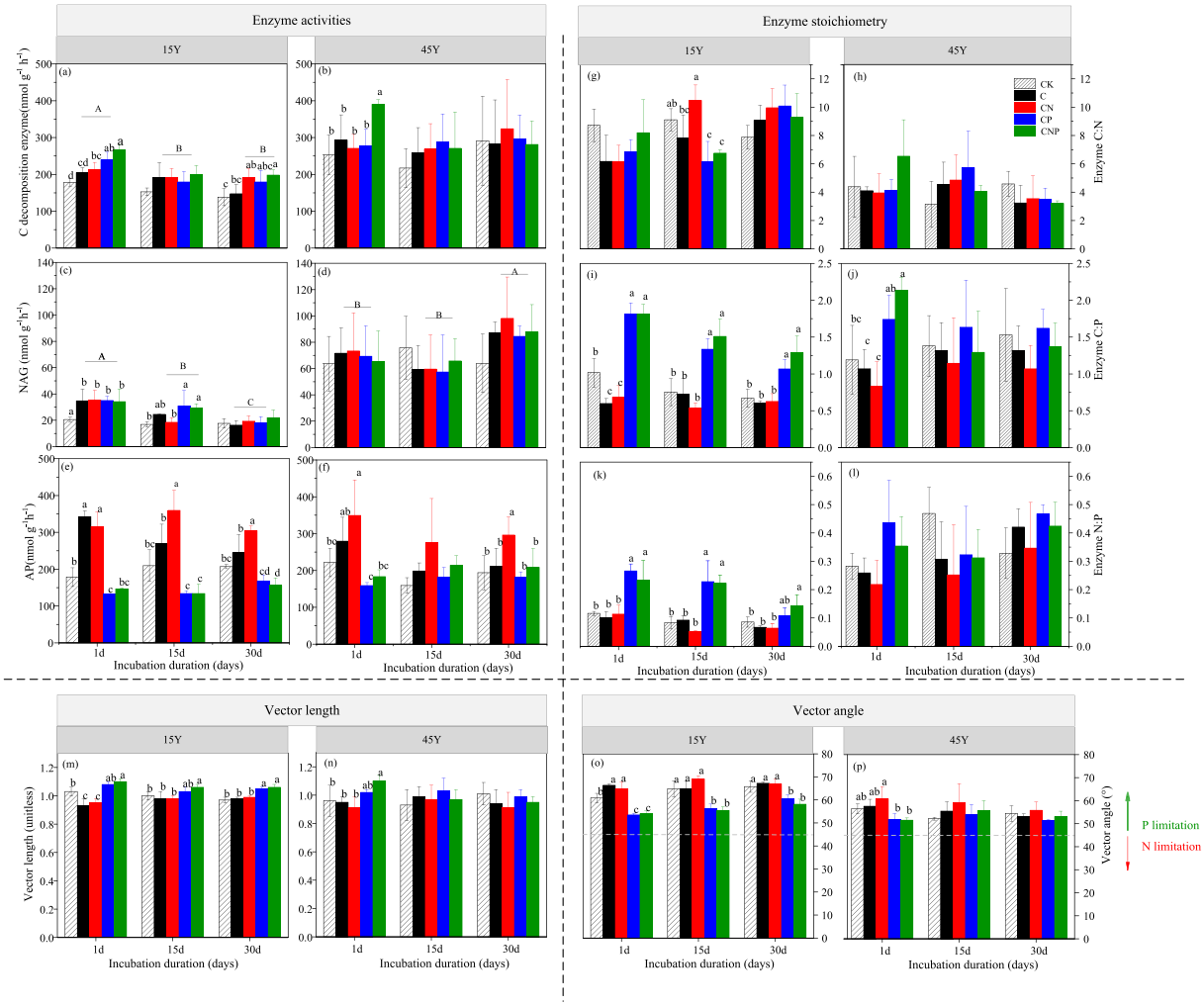

Fig. 5. Effects of glucose and nutrient additions on soil extracellular enzyme activities (a-f), enzyme stoichiometry (g-l) and microbial metabolic limitation (m-p) during three sampling periods. (a)-(b) Carbon decomposition enzymes (including β-1,4-glucosidase (BG) and cellobiohydrolase (CBH)); (c)-(d) β-1,4-N-acetyl-glucosaminidase (NAG); (e)-(f) alkaline phosphatase (AP). (g-h) Enzyme C:N, carbon decomposition enzymes/β-1,4-N-acetyl-glucosaminidase; (i-j) Enzyme C:P, carbon decomposition enzymes/alkaline phosphatase; (k-l) Enzyme N:P, β-1,4-N-acetyl-glucosaminidase/alkaline phosphatase at 15Y and 45Y, respectively. Vector length represents microbial relative C limitation, while vector angle represents N/P limitation of microbes (where $> 45°$ is microbial P limitation and $< 45°$ represents microbial N limitation). Values represent means ± standard deviations (n = 3). Lowercase letters indicate significant differences ($P < 0.05$) among the different nutrient treatments at the same sampling time.

3.2. Priming effect on SOC mineralization

Glucose addition with or without nutrient treatment caused both positive and negative priming effects on native SOC mineralization over the 30-day study period (Fig. 2a-d). Opposing patterns were observed for PE in both 15Y and 45Y soils. The PE of the 15-year-old stand (15Y) changed from positive (0–15 days) to negative (15–30 days) (Fig. 2a). Conversely, after 0.5 days, glucose with or without nutrient treatment caused a negative priming effect in the 45-year-old stand (45Y), while positive priming was observed after 1 day (except for glucose in combination with N treatment from 15 to 30 days) (Fig. 2b). The PE values of days 0–1 were significantly higher than those of days 1–15 and 15–30 (Fig. 2c-d). Stand age and nutrient treatment had a significantly positive effect on the cumulative PE at the end of the incubation ($P < 0.05$, Table S2, Fig. 2e-h). The older stand (45Y) had a higher cumulative PE than the younger stand (15Y). Glucose with N or NP addition decreased the cumulative PE compared with glucose addition alone ($P < 0.05$, Fig. 2g-h). The relative PE followed a very similar pattern between the stands and among the nutrient treatments (Fig. S1, Table S2).

3.3. Net C balance

The direction and magnitude of the net soil C balance were influenced by stand age and nutrient treatment (Fig. 3, Table S2). In total, 0.08–0.19 mg C g^{-1} glucose was recovered in SOC (glucose-derived SOC) on day 30 after glucose addition in the 15Y stand (Fig. 3a), and this quantity counterbalanced SOC loss and led to net C gains (0.02–0.17 mg C g^{-1} soil) (Fig. 3c). In contrast, lower glucose-derived SOC with a higher cumulative priming effect resulted in significant net C losses in the 45Y stand (except in the CN treatment, which had a net C gain in the 45Y stand) (Fig. 2f, h and Fig. 3b, d). Moreover, glucose in combination with N treatment resulted in a positive soil C balance regardless of stand age, which favoured soil C sequestration (Fig. 3 c-d).

3.4. Soil nutrient and enzyme activity dynamics

Stand age, nutrient treatment and incubation duration significantly influenced the available soil nutrients (Table S3). Glucose addition (C, CN, CP, and CNP) significantly increased soil C availability on days 1 and 30 compared to the control (Fig. 4a-b). The addition of CN and CNP significantly promoted N availability in 45Y (Fig. 4d, Table S3). The

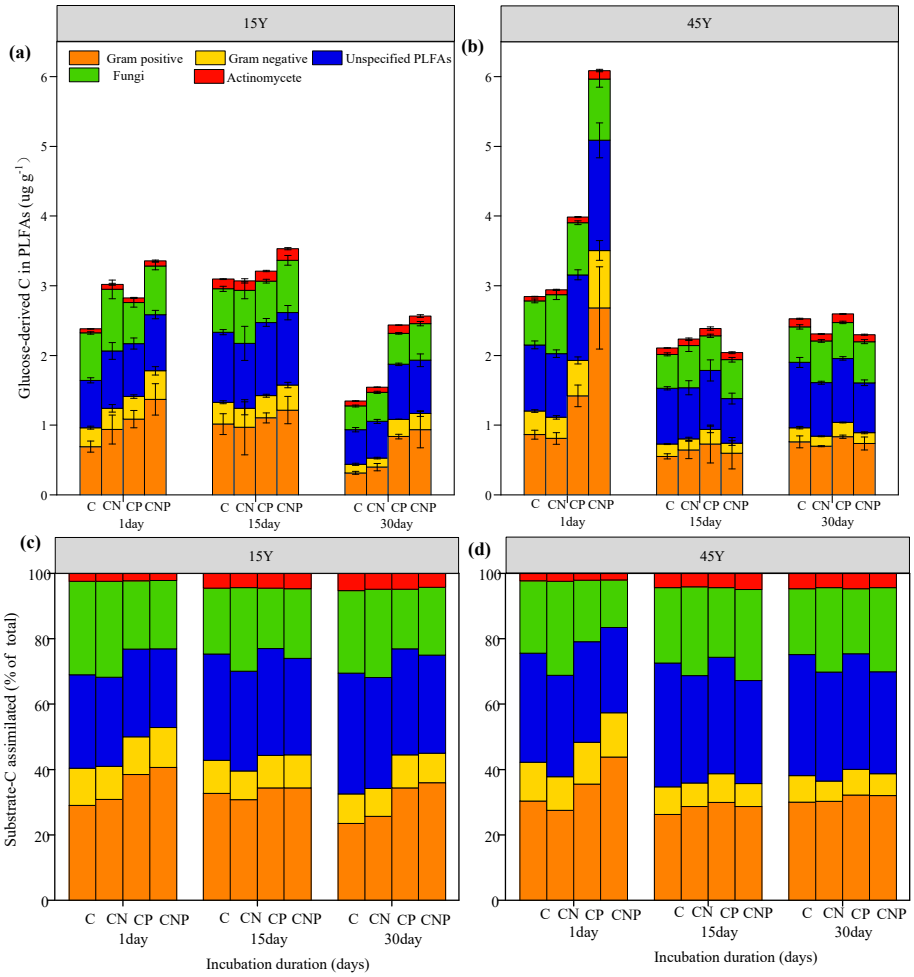

Fig. 6. Incorporation of glucose-derived ^{13}C into gram-positive bacteria, gram-negative bacteria, unspecified PLFAs, fungi and actinomycete PLFAs in 15Y and 45Y soil (a-b). Relative proportion (as % of total substrate incorporation into all PLFAs) of C substrate assimilated into PLFA biomarkers indicative of key microbial functional groups (c-d) with glucose (C) in combination with nutrient treatment (C, CN, CP and CNP). Data represent means ± SDs (n = 3). Bacterial PLFAs include gram-positive bacteria and gram-negative bacteria. Total PLFAs represent bacteria, fungi, actinomycetes and unspecified PLFAs. Data are expressed as the means ± SDs (n = 3).

contents of NH_4^+-N decreased (Fig. 4c-d), whereas the stoichiometric ratios of DOC/NH_4^+-N and DOC/SAP increased with incubation duration (Table S3). P addition significantly increased soil P availability (Fig. 4 e-f), which increased by 1.9–4.0 times under CP addition in 15Y and increased it by 1.1–3.3 times in 45Y under CNP addition compared with CK. P addition significantly decreased the soil stoichiometries of DOC/SAP and NH_4^+-N/SAP (Fig. 4i-l).

Stand age and nutrient treatment significantly influenced hydrolase activities, enzyme stoichiometry and vector length and angle (Table S4). Higher hydrolytic enzyme activities were measured in the older stand. Glucose addition significantly stimulated the activities of CBH + BG and NAG compared with CK at 15Y (Fig. 5a, c), while the CP and CNP treatments inhibited AP activity (Fig. 5e). Compared with glucose addition alone, the addition of CP and CNP increased the enzyme C:P, enzyme N:P and vector length but decreased the vector angle in the 15Y stand (Fig. 5i-p, Table. S4).

3.5. Total PLFAs and incorporation of ^{13}C into PLFAs

Stand age had a significant effect on soil total PLFAs (Fig. S2, Table S5), and nutrient treatment and incubation duration had significant effects on the total PLFAs and ^{13}C-bacteria PLFAs (Table S5). The incorporation of glucose-derived C into ^{13}C-bacteria PLFAs declined, while ^{13}C-actinomycete PLFAs increased with incubation duration (Fig. 6a-b, Table S5). The incorporation of glucose-derived C into bacterial PLFAs (31–59%) was greater than that of fungal PLFAs (13–32%) (Fig. 6c-d). Glucose with P or NP addition significantly increased glucose-derived C assimilation by gram-positive bacteria. Fungi assimilated a greater proportion of glucose in the CN addition treatment than in the glucose addition alone treatment in both stands (Fig. 6c-d).

Stand age, nutrient treatment and incubation duration had a significant effect on CUE and the microbial turnover rate (Table S5). The microbial CUE was higher in the 15Y stand than in the 45Y stand. The CUE decreased with incubation duration. The CN treatment had a relatively higher CUE than the C addition alone treatment (Table S5, Fig. 7a-b). P addition (CP and CNP treatments) increased bacterial turnover and decreased the fungal turnover rate on day 1 (Fig. 7c-d). CN addition increased the fungal turnover rate and decreased the bacterial turnover rate at 45Y on days 1 and 30 (Fig. 7d, f). The microbial turnover rate decreased with incubation time.

3.6. SEM analysis of the drivers of the priming effect

Correlation analysis showed that the cumulative PE was positively correlated with CO_2 emissions and enzyme N:P but was negatively correlated with VA, CUE and ^{13}C-PLFAs (Fig. 8).

SEM revealed the potential drivers of soil cumulative PE based on possible contributors of nutrient addition, microbial characteristics, soil and enzyme stoichiometry ($\chi^2 = 3.116$, df = 4, $P = 0.539$, RMSEA = 0.000, GFI = 0.986, SRMR = 0.04). The models accounted for 58% of the variation in PE (Fig. 9). Nutrient addition had a direct negative influence on PE (-0.52). Soil available C:N:P stoichiometry, $^{13}CO_2$ efflux, and ^{13}C-PLFAs had a direct positive influence on PE (0.48, 0.48, 0.23, respectively) (Fig. 9).

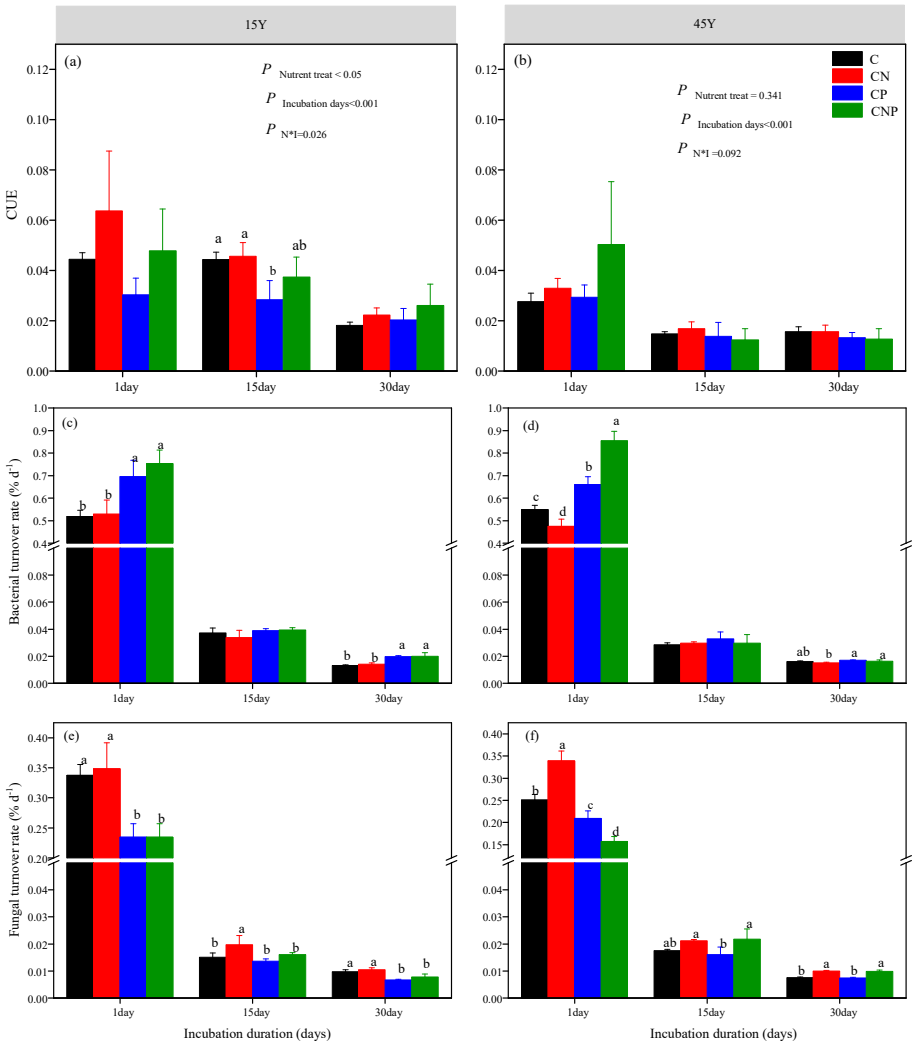

Fig. 7. Microbial C use efficiency (^{13}C incorporation in PLFAs relative to the sum of ^{13}C incorporation in PLFAs and ^{13}C released as CO_2) in 15Y and 45Y soils (a-b). Turnover rate of bacterial and fungal PLFAs in 15Y and 45Y soils at 1, 15, and 30 days (c-f). Data are expressed as the means ± SDs (n = 3).

4. Discussion

4.1. Priming effect in response to incubation times and microbial mechanisms

We observed that the direction of PE could be divided into two stages, which showed an opposite variation for the 15Y and 45Y stands. From 0 to 15 days, glucose addition induced a positive PE in the 15Y stand. Then, the positive PE changed to a negative PE on days 15–30 (Fig. 2a and c). Most microorganisms are dormant due to limited C availability; therefore, labile C inputs accelerate microbial activities and SOC mineralization for acquiring N (Xiao et al., 2021; Zhao et al., 2022). In our study, the positive PE (0–15 days) after glucose addition may be the result of "microbial stoichiometric decomposition" (Chen et al., 2014; Fang et al., 2018; Feng et al., 2021). This interpretation is supported by the C and N extracellular enzyme activities (Fig. 5a-c) increasing in all glucose addition treatments compared with the CK and the positive relationship between glucose-derived $^{13}CO_2$ and PE (Fig. 8). However, from 15 to 30 days, the increased NH_4^+-N concentration and decreased NAG extracellular enzyme activity demonstrated that the microbial allocation of N-acquiring enzymes was reduced (Fig. 4c and Fig. 5c), which indicated that microbial N limitation was alleviated. Therefore, PE declined in this period by reducing microbial nutrient mining (Fang et al., 2018).

In the early stage of the 45Y stand (0.5 days), the negative PE may be attributed to the preferential utilization of labile glucose relative to native SOM by soil microorganisms (Bei et al., 2022). C availability triggered microbial activity after 1 day, so glucose and nutrient addition better matched the microbial demand for carbon and nutrients and then promoted organic matter mineralization ("microbial stoichiometric decomposition"), which led to a positive priming effect (Zhang et al., 2021). The NAG activity increased after 15 days (Fig. 5d), which illustrated that microorganisms increased N mining, so a positive priming effect still occurred ("microbial N mining") (Zhu et al., 2021). These findings are consistent with our first hypothesis. Overall, our study provides evidence that different microbial mechanisms can operate at different stages and that they can coexist in a system to influence the priming effect.

As the magnitude of the priming effect varied, microbial succession also occurred at different stages. Our study showed that the ^{13}C-bacteria PLFA (r-strategists) proportion declined while ^{13}C-actinomycete (k-strategists) PLFAs increased with incubation duration (Fig. 6c-d), which is consistent with the finding of a DNA-SIP study indicating that bacteria were rapid responders to labile rice carbon in the early incubation stage, while actinobacteria gradually increased in the late incubation stage (Kong et al., 2020). R-strategies have advantages in decomposing labile carbon. Fungi and actinobacteria are mainly composed of k-strategists (Cui et al., 2020). K-strategists adapt to nutrient-deficient environments

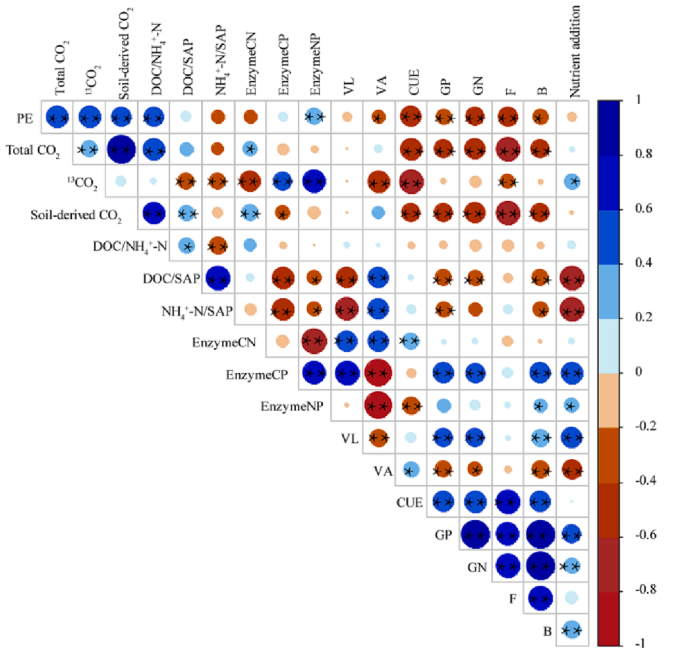

Fig. 8. Correlation analysis of the cumulative priming effect with CO_2 emissions, available CNP stoichiometry, enzyme CNP stoichiometry and microbial metabolic limitation, CUE, and ^{13}C-PLFAs. Blue indicates a positive correlation, red indicates a negative correlation, and the colour depth indicates the pearson coefficient. * and ** represent $P < 0.05$ and $P < 0.01$, respectively. PE, cumulative priming effect; Total CO_2, cumulative CO_2 release over the 30-day incubation; $^{13}CO_2$, cumulative glucose-derived CO_2 release over the 30-day incubation; Soil-derived CO_2, cumulative soil-derived CO2 release over the 30-day incubation; DOC/NH_4^+-N, soil dissolved organic carbon to ammoniacal nitrogen; DOC/SAP, soil dissolved organic carbon to soil available phosphorus ratio; NH_4^+-N/SAP, soil ammoniacal nitrogen to soil available phosphorus ratio; EnzymeCN, ratios of the activities of β-glucosidase (BG) plus β-cellobiohydrolase (CHB) to that of chitinase (NAG); EnzymeCP, ratios of the activities of β-glucosidase (BG) plus β-cellobiohydrolase (CHB) to that of phosphatase (AP); EnzymeNP, activity of NAG to that of AP; VL, vector length (relative C limitation); VA, vector angle (microbial N/P limitation); CUE, C use efficiency; GP, GN, F and B represent ^{13}C gram-positive bacteria, ^{13}C gram-negative bacteria, ^{13}C fungi and ^{13}C bacteria PLFA.

by generating extracellular enzymes to decompose recalcitrant carbon (Bei et al., 2022; Deng et al., 2020; Fontaine et al., 2003). Therefore, labile carbon input (high C availability) activates the r-strategy at the early stage; accordingly, this phenomenon described in 'microbial stoichiometric decomposition' can be ascribed to the contribution of the r-strategy (Chen et al., 2014). When labile C is gradually exhausted, microorganisms need to mine SOM to acquire nutrients for microbial growth, and the 'microbial N mining' theory is explained by the domination of the k-strategy (Chen et al., 2014). 'Preferential substrate utilization' theory can be used to explain the occurrence of a negative PE in the 45Y stand at the beginning of incubation (Blagodatskaya et al., 2007; Blagodatskaya and Kuzyakov, 2008; Deng et al., 2020).

Generally, fungi metabolize recalcitrant C more efficiently (Chen et al., 2022). However, we did not observe a significant increase in the fungal content in the late incubation stage (Fig. 6), which is inconsistent with findings reported by Zhang et al. (2021). The difference could possibly be explained by the lower incubation time in our study. Fungi have a lower assimilation of ^{13}C-glucose than bacteria (Fig. 6c-d), which also agrees with previous studies in which the fungal assimilation of glucose-derived ^{13}C was lower than bacterial assimilation (Wang et al., 2014; Zhang et al., 2021). This could be because fungi have a lower turnover rate than bacteria (Fig. 7c-f) (Gunina et al., 2017).

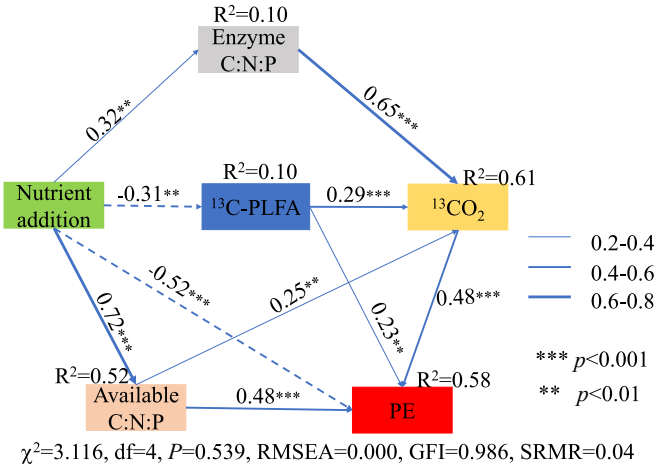

Fig. 9. Direct and indirect effects of C:N:P stoichiometry and $^{13}CO_2$ and microbial activity on priming effects based on structural equation modelling. Arrow width indicates the strength of the standardized path coefficient; solid and dotted lines indicate positive and negative path coefficients, respectively. R^2 values represent the proportion of variance of each endogenous variable. Nutrient addition: four levels (C, CN, CP and CNP); Enzyme C:N:P, ratios of enzyme CN, enzyme CP and enzyme NP. Available C:N:P, ratios of DOC, NH_4^+-N and SAP. *, **, and *** represent correlations that are significant at $P < 0.05$, $P < 0.01$ and $P < 0.001$, respectively.

4.2. *Cumulative priming effect in response to glucose and nutrient addition*

Glucose input provides available C to stimulate microbial growth. Our results showed that ^{13}C-glucose addition resulted in a positive cumulative priming effect in *Robinia pseudoacacia* soil after 30 days of incubation. Similarly, previous studies have demonstrated that labile carbon stimulates soil organic matter decomposition, which is attributed to the priming effect (Chen et al., 2022; Zhao et al., 2022; Zhou et al., 2022b). Nitrogen-mineralizing enzyme activities (NAG) increased after glucose addition in 15Y at days 1–15 (Fig. 5c), which means a relatively large investment in nitrogen acquisition, confirming the 'microbial N mining' hypothesis. This theory indicates that after the addition of a labile carbon source, microorganisms use the energy in labile carbon to decompose more recalcitrant C to obtain N (Fontaine et al., 2003). In addition, labile C input may trigger the microbial community and promote fast-growing microbial community proliferation, therefore stimulating organic carbon decomposition (Fanin et al., 2020; Razanamalala et al., 2017).

In our study, the amount of substrate C addition was the same for all treatments. Therefore, the difference in the cumulative priming effect in different soils was attributed to nutrient addition. Indeed, our results showed that the magnitude of the cumulative PE was significantly influenced by nutrient addition (Table S2, Fig. 9) but was not completely consistent with our second hypothesis. Compared to glucose-derived C addition alone, glucose-derived C plus N addition (CN and CNP addition) significantly decreased soil-derived CO_2 emissions and the cumulative PE. Previous studies have indicated that nitrogen addition decreases the priming effect (Chen et al., 2018; Chen et al., 2014; Feng and Zhu, 2021; Hicks et al., 2019). Our study indicated that fungi assimilated a greater proportion of glucose in the CN addition treatment (Fig. 6c-d). Increased nitrogen availability may alleviate fungal N requirements (Liu et al., 2013), decrease microbial N mining from SOM and inhibit recalcitrant SOM decomposition (Du et al., 2020; Fang et al., 2018). However, CP addition had no significant influence on the cumulative PE compared to glucose-derived C addition alone. This suggests that the priming effect in these soils may not be determined by microbial P demand (Hicks et al., 2019). The absence of an effect of phosphorus addition on the priming effect may reflect the many ways for

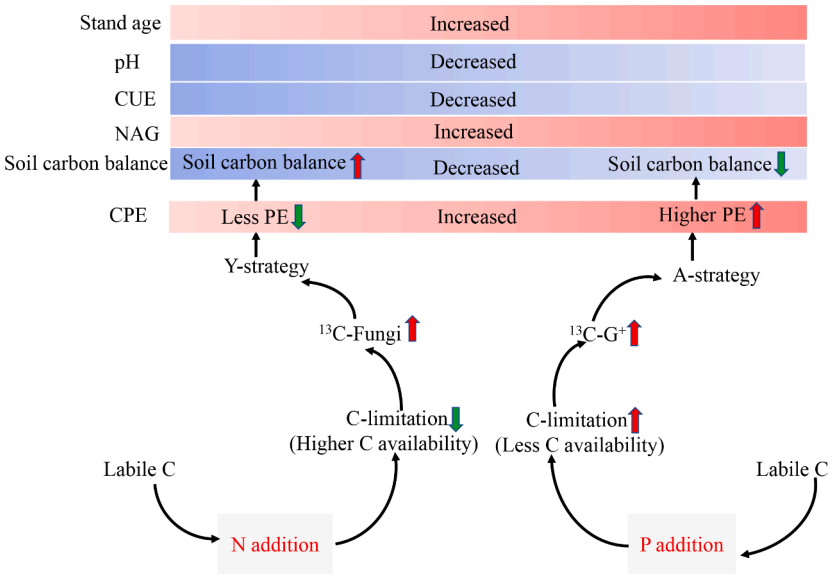

Fig. 10. Changes in the cumulative priming effect and soil carbon balance at different stand ages and nutrient additions. Higher pH and CUE and lower NAG enzyme activities in 15Y led to a lower cumulative priming effect but a higher soil carbon balance. Older stand ages (45Y) showed the opposite trend. In both 15Y and 45Y, N addition decreased the cumulative PE and resulted in soil net carbon gains. Nitrogen addition alleviated microbial C limitation and increased the assimilation of ^{13}C-glucose by fungi, which shifted the microbial community to the Y-strategy. In contrast, P addition exacerbated microbial C limitation and increased the assimilation of ^{13}C-glucose by gram-positive bacteria, which shifted the microbial community to the A-strategy. Increasing SOC mineralization leads to a higher cumulative priming effect and lower soil carbon balance. CUE: microbial carbon use efficiency; CPE: cumulative priming effect.

microbes to acquire P, such as the acquisition of P from biochemical hydrolysis and inorganic sources (Hicks et al., 2019; McGill and Cole, 1981).

4.3. Cumulative priming effect in response to stand age

We found that the cumulative PE in the 45Y soil was greater than that in the 15Y soil (Fig. 2g-h), which is inconsistent with the finding of a recent study indicating that cumulative PE initially increased to a peak value and declined thereafter along an afforestation chronosequence (Zhou et al., 2022b). The different outcomes in our study may be caused by the different stand ages and incomplete restoration chronosequence. Many studies have indicated that the SOC content, pH and enzyme activities are drivers of cumulative PE (Bastida et al., 2019; Ren et al., 2021). Previous studies demonstrated that cumulative PE was negatively correlated with the SOC content (Feng et al., 2021; Zhao et al., 2022). In contrast with our third hypothesis, there was a higher SOC content in the 45Y stand, but the cumulative PE was higher in the 45Y stand than in the 15Y stand, which suggests that the SOC content in our study was not the main regulator of the cumulative PE. In our study, the greater cumulative PE in the 45Y stand may be attributed to three pieces of evidence. First, the cumulative PE was negatively correlated with the pH value (Xiao et al., 2021). It has been reported that initial soil pH can regulate the PE by influencing microbial abundance and community composition (Aye et al., 2018; Chen et al., 2022). In our study, the total microbial PLFAs were higher at 45Y (pH = 6.68) than at 15Y (pH = 7.97) (Fig. S2), and the PE may be enhanced by higher microbial biomass and activity in older stands (Aye et al., 2017). Therefore, the higher cumulative PE in the 45Y stand may be related to its lower pH value. Second, higher NAG activity was observed in the 45Y stand (Fig. 5d), which indicated that this stand was N-limited. Previous studies have demonstrated that P limitation also increases with increasing stand age (Zhang et al., 2019; Zhong et al., 2020). Therefore, ^{13}C-glucose addition activated microbes to mineralize SOM to meet their nutrient demand, which resulted in a greater cumulative PE. Finally, the greater cumulative PE in the 45Y stand may be related to lower microbial carbon use efficiency (CUE) (Fig. 7b, Table S5). Many studies have indicated that the cumulative PE is negatively correlated with CUE (Liao et al., 2020; Mo et al., 2021a; Mo et al., 2021b). This finding is supported by correlation analysis of the cumulative priming effect and microbial carbon use efficiency (Fig. 8).

4.4. Accumulation of glucose-derived C and the soil net C balance

The soil C balance is regulated by SOC accumulation by increasing microbial biomass and SOC mineralization via microbial decomposition (Blagodatskaya and Kuzyakov, 2008; Zhu et al., 2022). In our study, the highest positive net C balance in the soil was obtained through CN addition, suggesting that nitrogen addition was conducive to carbon accumulation. Microbial growth could be one possible explanation. The total PLFAs were lower under CN addition than in CK at the end of incubation. The lower microbial growth and activity under the CN treatment may not enhance the decomposition of SOM and the generation of a PE, which is conducive to soil carbon sequestration. This is in accordance with Huang et al. (2020), who found that nitrogen addition stimulated soil C storage by both increasing soil C input and decreasing the decomposition of old soil C. Vector length analysis showed that CN addition alleviated microbial C limitation compared to CK (Fig. 5m), indicating that the absence of resource limitation is expected to favour the high-yield strategy (Y-strategy) (Malik et al., 2019a). This was supported by a higher CUE and glucose-derived C accumulation under CN addition. In contrast, vector analysis showed that CP addition increased microbial C limitation and alleviated microbial P limitation (Fig. 5m-p). A recent study indicated that decreasing microbial phosphorus limitation increases soil carbon release (Cui et al., 2022). As a result, CP addition increases ^{13}C-G^{+} bacterial abundance (Fig. 6a-b), drives the microbial community to an A-strategy by accelerating SOC decomposition for C or nutrient resource acquisition, and decreases glucose-derived SOC accumulation and net C balance (Malik et al., 2019b; Shao et al., 2021; Zhu et al., 2022). Our study indicated that the microbial community can adjust its life strategy to respond to carbon and nutrient conditions (Fig. 10). The response of microbial life strategies to N and P addition affects the soil carbon balance.

Compared with the 45Y soil, the 15Y soil had a positive net C balance. This is probably because a higher CUE, glucose-derived SOC accumulation, lower C and N hydrolase and positive PE were observed in the 15Y soil. This means that the increase in glucose-derived SOC exceeded the soil SOC loss and led to net SOC accumulation after glucose addition. However, due to our short incubation time (30 days), the result may be temporary. Glucose-derived compounds have a longer mean residence time than glucose molecules themselves and continue to stimulate microorganisms to decompose native SOM (Fontaine et al., 2004; Li et al., 2020; Zhou et al., 2022a). Finally, the added glucose might be exhausted, and SOC decomposition continues for a long time and leads to net C loss.

5. Conclusions

In this study, we explored how carbon and nutrient addition influenced the cumulative priming effect and soil carbon balance of *Robinia pseudoacacia* stands of different ages. The priming effect induced by carbon and nutrient addition had an obvious temporal dynamic. 'Stoichiometry decomposition' theory dominated the priming effect at the early stage, while the 'microbial N mining' mechanism explained more of the priming effect at the late stage. Both stands had a positive cumulative priming effect at the end of the 30-day incubation, and the older stand had a greater cumulative priming effect than the younger stand. The cumulative priming effect decreased with N addition, but there was no significant influence of P addition. In addition, CN addition (alleviation of microbial C limitation) increased the incorporation of ^{13}C-glucose into fungi and shifted the microbial community to a high-yielding strategy (Y strategy), leading to a positive net C balance. CP addition (an increase in microbial C limitation) increased the incorporation of ^{13}C-glucose into gram-positive bacteria, shifted the microbial community to a resource acquisition strategy (A-strategy), and then decreased the soil C balance. Therefore, the soil microorganism life strategy can change in response to carbon and nutrient availability to regulate the PE and soil carbon balance.

Declaration of Competing Interest

The authors declare that they have no known competing financial interests or personal relationships that could have appeared to influence the work reported in this paper.

Data availability

Data will be made available on request.

Acknowledgements

This work was supported by the Science and Technology Innovation Program of the Shaanxi Academy of Forestry (SXLK2022-02-03), and the National Natural Science Foundation of China (42077452).

Appendix A. Supplementary data

Supplementary data to this article can be found online at https://doi.org/10.1016/j.geoderma.2023.116444.

References

Aye, N.S., Butterly, C.R., Sale, P.W., Tang, C., 2017. Residue addition and liming history interactively enhance mineralization of native organic carbon in acid soils. Biol. Fertil. Soils 53 (1), 61–75. https://doi.org/10.1007/s00374-016-1156-y.

Aye, N.S., Butterly, C.R., Sale, P.W., Tang, C., 2018. Interactive effects of initial pH and nitrogen status on soil organic carbon priming by glucose and lignocellulose. Soil Biol. Biochem. 123, 33–44. https://doi.org/10.1016/j.soilbio.2018.04.027.

Bao, S.D., 2000. Soil and Agricultural Chemistry Analysis. China Agriculture Press, Beijing, China (in Chinese).

Bastida, F., García, C., Fierer, N., Eldridge, D.J., Bowker, M.A., Abades, S., Alfaro, F.D., Asefaw Berhe, A., Cutler, N.A., Gallardo, A., 2019. Global ecological predictors of the soil priming effect. Nat. Commun. 10 (1), 1–9. https://doi.org/10.1038/s41467-019-11472-7.

Bei, S., Li, X., Kuyper, T.W., Chadwick, D.R., Zhang, J., 2022. Nitrogen availability mediates the priming effect of soil organic matter by preferentially altering the straw carbon-assimilating microbial community. Sci. Total Environ. 815, 152882 https://doi.org/10.1016/j.scitotenv.2021.152882.

Blagodatskaya, E.V., Blagodatsky, S.A., Anderson, T.H., Kuzyakov, Y., 2007. Priming effects in Chernozem induced by glucose and N in relation to microbial growth strategies. Appl. Soil Ecol. 37 (1–2), 95–105. https://doi.org/10.1016/j.apsoil.2007.05.002.

Blagodatskaya, E., Kuzyakov, Y., 2008. Mechanisms of real and apparent priming effects and their dependence on soil microbial biomass and community structure: critical review. Biol. Fertil. Soils 45 (2), 115–131. https://doi.org/10.1007/s00374-008-0334-y.

Chen, Y., Li, W., You, Y., Ye, C., Shu, X., Zhang, Q., Zhang, K., 2022. Soil properties and substrate quality determine the priming of soil organic carbon during vegetation succession. Plant and Soil 471 (1–2), 559–575. https://doi.org/10.1007/s11104-021-05241-z.

Chen, L., Liu, L., Mao, C., Qin, S., Wang, J., Liu, F., Blagodatsky, S., Yang, G., Zhang, Q., Zhang, D., 2018. Nitrogen availability regulates topsoil carbon dynamics after permafrost thaw by altering microbial metabolic efficiency. Nat. Commun. 9 (1), 1–11. https://doi.org/10.1038/s41467-018-06232-y.

Chen, L., Liu, L., Qin, S., Yang, G., Fang, K., Zhu, B., Kuzyakov, Y., Chen, P., Xu, Y., Yang, Y., 2019. Regulation of priming effect by soil organic matter stability over a broad geographic scale. Nat. Commun. 10 (1), 1–10. https://doi.org/10.1038/s41467-019-13119-z.

Chen, R., Senbayram, M., Blagodatsky, S., Myachina, O., Dittert, K., Lin, X., Blagodatskaya, E., Kuzyakov, Y., 2014. Soil C and N availability determine the priming effect: microbial N mining and stoichiometric decomposition theories. Glob. Chang. Biol. 20 (7), 2356–2367. https://doi.org/10.1111/gcb.12475.

Craine, J.M., Morrow, C., Fierer, N., 2007. Microbial nitrogen limitation increases decomposition. Ecology 88 (8), 2105–2113. https://doi.org/10.1890/06-1847.1.

Cui, Y., Moorhead, D.L., Wang, X., Xu, M., Wang, X., Wei, X., Zhu, Z., Ge, T., Peng, S., Zhu, B., Zhang, X., Fang, L., 2022. Decreasing microbial phosphorus limitation increases soil carbon release. Geoderma 419, 115868. https://doi.org/10.1016/j.geoderma.2022.115868.

Cui, J., Zhu, Z., Xu, X., Liu, S., Jones, D.L., Kuzyakov, Y., Shibistova, O., Wu, J., Ge, T., 2020. Carbon and nitrogen recycling from microbial necromass to cope with C: N stoichiometric imbalance by priming. Soil Biol. Biochem. 142, 107720 https://doi.org/10.1016/j.soilbio.2020.107720.

DeForest, J.L., 2009. The influence of time, storage temperature, and substrate age on potential soil enzyme activity in acidic forest soils using MUB-linked substrates and L-DOPA. Soil Biol. Biochem. 41 (6), 1180–1186. https://doi.org/10.1016/j.soilbio.2009.02.029.

Deng, S., Zheng, X., Chen, X., Zheng, S., He, X., Ge, T., Kuzyakov, Y., Wu, J., Su, Y., Hu, Y., 2020. Divergent mineralization of hydrophilic and hydrophobic organic substrates and their priming effect in soils depending on their preferential utilization by bacteria and fungi. Biol. Fertil. Soils 57 (1), 65–76. https://doi.org/10.1007/s00374-020-01503-7.

Du, L., Zhu, Z., Qi, Y., Zou, D., Zhang, G., Zeng, X., Ge, T., Wu, J., Xiao, Z., 2020. Effects of different stoichiometric ratios on mineralisation of root exudates and its priming effect in paddy soil. Sci. Total Environ. 743, 140808 https://doi.org/10.1016/j.scitotenv.2020.140808.

Fang, Y., Nazaries, L., Singh, B.K., Singh, B.P., 2018. Microbial mechanisms of carbon priming effects revealed during the interaction of crop residue and nutrient inputs in contrasting soils. Glob. Chang. Biol. 24 (7), 2775–2790. https://doi.org/10.1111/gcb.14154.

Fanin, N., Hättenschwiler, S., Schimann, H., Fromin, N., Bailey, J.K., 2014. Interactive effects of C, N and P fertilization on soil microbial community structure and function in an Amazonian rain forest. Funct. Ecol. 29 (1), 140–150. https://doi.org/10.1111/1365-2435.12329.

Fanin, N., Moorhead, D., Bertrand, I., 2016. Eco-enzymatic stoichiometry and enzymatic vectors reveal differential C, N, P dynamics in decaying litter along a land-use gradient. Biogeochemistry 129 (1–2), 21–36. https://doi.org/10.1007/s10533-016-0217-5.

Fanin, N., Alavoine, G., Bertrand, I., 2020. Temporal dynamics of litter quality, soil properties and microbial strategies as main drivers of the priming effect. Geoderma 377, 114576. https://doi.org/10.1016/j.geoderma.2020.114576.

Feng, J., Tang, M., Zhu, B., 2021. Soil priming effect and its responses to nutrient addition along a tropical forest elevation gradient. Glob. Chang. Biol. 27 (12), 2793–2806. https://doi.org/10.1111/gcb.15587.

Feng, J., Zhu, B., 2021. Global patterns and associated drivers of priming effect in response to nutrient addition. Soil Biol. Biochem. 153, 108118 https://doi.org/10.1016/j.soilbio.2020.108118.

Fontaine, S., Mariotti, A., Abbadie, L., 2003. The priming effect of organic matter: a question of microbial competition? Soil Biol. Biochem. 35 (6), 837–843. https://doi.org/10.1016/S0038-0717(03)00123-8.

Fontaine, S., Bardoux, G., Abbadie, L., Mariotti, A., 2004. Carbon input to soil may decrease soil carbon content. Ecol. Lett. 7 (4), 314–320. https://doi.org/10.1111/j.1461-0248.2004.00579.x.

Fontaine, S., Henault, C., Aamor, A., Bdioui, N., Bloor, J.M.G., Maire, V., Mary, B., Revaillot, S., Maron, P.A., 2011. Fungi mediate long term sequestration of carbon and nitrogen in soil through their priming effect. Soil Biol. Biochem. 43 (1), 86–96. https://doi.org/10.1016/j.soilbio.2010.09.017.

Fu, X., Song, Q., Li, S., Shen, Y., Yue, S., 2022. Dynamic changes in bacterial community structure are associated with distinct priming effect patterns. Soil Biol. Biochem. 108671 https://doi.org/10.1016/j.soilbio.2022.108671.

Gunina, A., Dippold, M., Glaser, B., Kuzyakov, Y., 2017. Turnover of microbial groups and cell components in soil: ^{13}C analysis of cellular biomarkers. Biogeosciences 14 (2), 271–283. https://doi.org/10.5194/bg-14-271-2017.

Hicks, L.C., Meir, P., Nottingham, A.T., Reay, D.S., Stott, A.W., Salinas, N., Whitaker, J., 2019. Carbon and nitrogen inputs differentially affect priming of soil organic matter in tropical lowland and montane soils. Soil Biol. Biochem. 129, 212–222. https://doi.org/10.1016/j.soilbio.2018.10.015.

Huang, X., Terrer, C., Dijkstra, F.A., Hungate, B.A., Zhang, W., van Groenigen, K.J., 2020. New soil carbon sequestration with nitrogen enrichment: a meta-analysis. Plant Soil 454 (1–2), 299–310. https://doi.org/10.1007/s11104-020-04617-x.

Jackson, R.B., Lajtha, K., Crow, S.E., Hugelius, G., Kramer, M.G., Piñeiro, G., 2017. The Ecology of Soil Carbon: Pools, Vulnerabilities, and Biotic and Abiotic Controls. Annu. Rev. Ecol. Evol. Syst. 48 (1), 419–445. https://doi.org/10.1146/annurev-ecolsys-112414-054234.

Jandl, R., Lindner, M., Vesterdal, L., Bauwens, B., Baritz, R., Hagedorn, F., Johnson, D. W., Minkkinen, K., Byrne, K.A., 2007. How strongly can forest management influence soil carbon sequestration? Geoderma 137 (3–4), 253–268. https://doi.org/10.1016/j.geoderma.2006.09.003.

Jing, H., Liu, Y., Wang, G., Liu, G., 2021. Contrasting effects of nitrogen addition on rhizosphere soil CO_2, N_2O, and CH_4 emissions of fine roots with different diameters from Pinus tabulaeformis forest using laboratory incubation. Sci. Total Environ. 780, 146298 https://doi.org/10.1016/j.scitotenv.2021.146298.

Kong, Y., Kuzyakov, Y., Ruan, Y., Zhang, J., Wang, T., Wang, M., Guo, S., Shen, Q., Ling, N., Vieille, C., 2020. DNA Stable-Isotope Probing Delineates Carbon Flows from Rice Residues into Soil Microbial Communities Depending on Fertilization. Appl. Environ. Microbiol. 86 (7) https://doi.org/10.1128/AEM.02151-19.

Kuzyakov, Y., 2010. Priming effects: Interactions between living and dead organic matter. Soil Biol. Biochem. 42 (9), 1363–1371. https://doi.org/10.1016/j.soilbio.2010.04.003.

Kuzyakov, Y., Friedel, J., Stahr, K., 2000. Review of mechanisms and quantification of priming effects. Soil Biol. Biochem. 32 (11–12), 1485–1498. https://doi.org/10.1016/S0038-0717(00)00084-5.

Li, J., Xie, J., Zhang, Y., Dong, L., Shangguan, Z., Deng, L., 2022. Interactive effects of nitrogen and water addition on soil microbial resource limitation in a temperate desert shrubland. Plant and Soil 1–18. https://doi.org/10.1007/s11104-022-05371-y.

Li, J.H., Zhang, R., Cheng, B.H., Ye, L.F., Li, W.J., Shi, X.M., 2020. Effects of nitrogen and phosphorus additions on decomposition and accumulation of soil organic carbon in alpine meadows on the Tibetan Plateau. Land Degrad. Dev. 32 (3), 1467–1477. https://doi.org/10.1002/ldr.3792.

Li, L.-J., Zhu-Barker, X., Ye, R., Doane, T.A., Horwath, W.R., 2018. Soil microbial biomass size and soil carbon influence the priming effect from carbon inputs depending on nitrogen availability. Soil Biol. Biochem. 119, 41–49. https://doi.org/10.1016/j.soilbio.2018.01.003.

Liao, C., Tian, Q., Liu, F., 2020. Nitrogen availability regulates deep soil priming effect by changing microbial metabolic efficiency in a subtropical forest. J. For. Res. 32 (2), 713–723. https://doi.org/10.1007/s11676-020-01148-0.

Liu, Y., Fang, Y., An, S., 2020. How C: N: P stoichiometry in soils and plants responds to succession in Robinia pseudoacacia forests on the Loess Plateau, China. Forest Ecol. Manage. 475, 118394 https://doi.org/10.1016/j.foreco.2020.118394.

Liu, J., Wang, Q., Ku, Y., Zhang, W., Zhu, H., Zhao, Z., 2022. Precipitation and soil pH drive the soil microbial spatial patterns in the Robinia pseudoacacia forests at the regional scale. Catena 212, 106120. https://doi.org/10.1016/j.catena.2022.106120.

Liu, L., Zhang, T., Gilliam, F.S., Gundersen, P., Zhang, W., Chen, H., Mo, J., 2013. Interactive Effects of Nitrogen and Phosphorus on Soil Microbial Communities in a Tropical Forest. PLoS One 8 (4), e61188.

Malik, A.A., Martiny, J.B.H., Brodie, E.L., Martiny, A.C., Treseder, K.K., Allison, S.D., 2019a. Defining trait-based microbial strategies with consequences for soil carbon cycling under climate change. ISME J. 14 (1), 1–9. https://doi.org/10.1038/s41396-019-0510-0.

Malik, A.A., Puissant, J., Goodall, T., Allison, S.D., Griffiths, R.I., 2019b. Soil microbial communities with greater investment in resource acquisition have lower growth yield. Soil Biol. Biochem. 132, 36–39. https://doi.org/10.1016/j.soilbio.2019.01.025.

McGill, W., Cole, C., 1981. Comparative aspects of cycling of organic C, N, S and P through soil organic matter. Geoderma 26 (4), 267–286. https://doi.org/10.1016/0016-7061(81)90024-0.

Mo, C., Jiang, Z., Chen, P., Cui, H., Yang, J., 2021a. Microbial metabolic efficiency functions as a mediator to regulate rhizosphere priming effects. Sci. Total Environ. 759, 143488 https://doi.org/10.1016/0016-7061(81)90024-0.

Mo, F., Zhang, Y.-Y., Liu, Y., Liao, Y.-C., 2021b. Microbial carbon-use efficiency and straw-induced priming effect within soil aggregates are regulated by tillage history and balanced nutrient supply. Biol. Fertil. Soils 57 (3), 409–420. https://doi.org/10.1007/s00374-021-01540-w.

Mo, F., Ren, C., Yu, K., Zhou, Z., Phillips, R.P., Luo, Z., Zhang, Y., Dang, Y., Han, J., Ye, J. S., 2022. Global pattern of soil priming effect intensity and its environmental drivers. Ecology e3790. https://doi.org/10.1002/ecy.3790.

Moorhead, D.L., Sinsabaugh, R.L., Hill, B.H., Weintraub, M.N., 2016. Vector analysis of ecoenzyme activities reveal constraints on coupled C, N and P dynamics. Soil Biol. Biochem. 93, 1–7. https://doi.org/10.1016/j.soilbio.2015.10.019.

Nottingham, A.T., Hicks, L.C., Ccahuana, A.J.Q., Salinas, N., Bååth, E., Meir, P., 2017. Nutrient limitations to bacterial and fungal growth during cellulose decomposition in tropical forest soils. Biol. Fertil. Soils 54 (2), 219–228. https://doi.org/10.1007/s00374-017-1247-4.

Razanamalala, K., Razafimbelo, T., Maron, P.-A., Ranjard, L., Chemidlin, N., Lelièvre, M., Dequiedt, S., Ramaroson, V.H., Marsden, C., Becquer, T., Trap, J., Blanchart, E., Bernard, L., 2017. Soil microbial diversity drives the priming effect along climate gradients: a case study in Madagascar. ISME J. 12 (2), 451–462. https://doi.org/10.1038/ismej.2017.178.

Ren, C., Wang, J., Bastida, F., Delgado-Baquerizo, M., Yang, Y., Wang, J., Zhong, Z., Zhou, Z., Zhang, S., Guo, Y., Zhou, S., Wei, G., Han, X., Yang, G., Zhao, F., 2021. Microbial traits determine soil C emission in response to fresh carbon inputs in forests across biomes. Glob. Chang. Biol. 28 (4), 1516–1528. https://doi.org/10.1111/gcb.16004.

Ren, C., Mo, F., Zhou, Z., Bastida, F., Delgado-Baquerizo, M., Wang, J., Zhang, X., Luo, Y., Griffis, T.J., Han, X., Wei, G., Wang, J., Zhong, Z., Feng, Y., Ren, G., Wang, X., Yu, K., Zhao, F., Yang, G., Yuan, F., 2022. The global biogeography of soil priming effect intensity. Glob. Ecol. Biogeogr. 31 (8), 1679–1687. https://doi.org/10.1111/geb.13524.

Saiya-Cork, K., Sinsabaugh, R., Zak, D., 2002. The effects of long term nitrogen deposition on extracellular enzyme activity in an Acer saccharum forest soil. Soil Biol. Biochem. 34 (9), 1309–1315. https://doi.org/10.1016/S0038-0717(02)00074-3.

Scharlemann, J.P.W., Tanner, E.V.J., Hiederer, R., Kapos, V., 2014. Global soil carbon: understanding and managing the largest terrestrial carbon pool. Carbon Manage. 5 (1), 81–91. https://doi.org/10.4155/cmt.13.77.

Shao, P., Lynch, L., Xie, H., Bao, X., Liang, C., 2021. Tradeoffs among microbial life history strategies influence the fate of microbial residues in subtropical forest soils. Soil Biol. Biochem. 153, 108112 https://doi.org/10.1016/j.soilbio.2020.108112.

Sun, Z., Liu, S., Zhang, T., Zhao, X., Chen, S., Wang, Q., 2019. Priming of soil organic carbon decomposition induced by exogenous organic carbon input: a meta-analysis. Plant Soil 443 (1–2), 463–471. https://doi.org/10.1007/s11104-019-04240-5.

Van Zwieten, L., Kimber, S., Morris, S., Downie, A., Berger, E., Rust, J., Scheer, C., 2010. Influence of biochars on flux of N_2O and CO_2 from Ferrosol. Soil Res. 48 (7), 555–568. https://doi.org/10.1071/SR10004.

Wang, Q., Wang, S., He, T., Liu, L., Wu, J., 2014. Response of organic carbon mineralization and microbial community to leaf litter and nutrient additions in subtropical forest soils. Soil Biol. Biochem. 71, 13–20. https://doi.org/10.1016/j.soilbio.2014.01.004.

Wu, L., Xu, H., Xiao, Q., Huang, Y., Suleman, M.M., Zhu, P., Kuzyakov, Y., Xu, X., Xu, M., Zhang, W., 2020. Soil carbon balance by priming differs with single versus repeated addition of glucose and soil fertility level. Soil Biol. Biochem. 148, 107913 https://doi.org/10.1016/j.soilbio.2020.107913.

Xiao, Q., Huang, Y., Wu, L., Tian, Y., Wang, Q., Wang, B., Xu, M., Zhang, W., 2021. Long-term manuring increases microbial carbon use efficiency and mitigates priming effect via alleviated soil acidification and resource limitation. Biol. Fertil. Soils 57 (7), 925–934. https://doi.org/10.1007/s00374-021-01583-z.

Yuan, H., Zhu, Z., Liu, S., Ge, T., Jing, H., Li, B., Liu, Q., Lynn, T.M., Wu, J., Kuzyakov, Y., 2016. Microbial utilization of rice root exudates: ^{13}C labeling and PLFA composition. Biol. Fertil. Soils 52 (5), 615–627. https://doi.org/10.1007/s00374-016-1101-0.

Zhang, Q., Cheng, L., Feng, J., Mei, K., Zeng, Q., Zhu, B., Chen, Y., 2021. Nitrogen addition stimulates priming effect in a subtropical forest soil. Soil Biol. Biochem. 160, 108339 https://doi.org/10.1016/j.soilbio.2021.108339.

Zhang, K., Ni, Y., Liu, X., Chu, H., 2020. Microbes changed their carbon use strategy to regulate the priming effect in an 11-year nitrogen addition experiment in grassland. Sci. Total Environ. 727, 138645 https://doi.org/10.1016/j.scitotenv.2020.138645.

Zhang, W., Xu, Y., Gao, D., Wang, X., Liu, W., Deng, J., Han, X., Yang, G., Feng, Y., Ren, G., 2019. Ecoenzymatic stoichiometry and nutrient dynamics along a revegetation chronosequence in the soils of abandoned land and *Robinia pseudoacacia* plantation on the Loess Plateau, China. Soil Biol. Biochem. 134, 1–14. https://doi.org/10.1016/j.soilbio.2019.03.017.

Zhao, F., Wang, J., Li, Y., Xu, X., He, L., Wang, J., Ren, C., Guo, Y., 2022. Microbial functional genes driving the positive priming effect in forest soils along an elevation gradient. Soil Biol. Biochem. 165, 108498 https://doi.org/10.1016/j.soilbio.2021.108498.

Zheng, Y., Jin, J., Wang, X., Clark, G.J., Tang, C., 2022. Increasing nitrogen availability does not decrease the priming effect on soil organic matter under pulse glucose and single nitrogen addition in woodland topsoil. Soil Biol. Biochem. 172, 108767 https://doi.org/10.1016/j.soilbio.2022.108767.

Zhong, Z., Li, W., Lu, X., Gu, Y., Wu, S., Shen, Z., Han, X., Yang, G., Ren, C., 2020. Adaptive pathways of soil microorganisms to stoichiometric imbalances regulate microbial respiration following afforestation in the Loess Plateau, China. Soil Biol. Biochem. 151, 108048 https://doi.org/10.1016/j.soilbio.2020.108048.

Zhou, S., Lin, J., Wang, P., Zhu, P., Zhu, B., 2022a. Resistant soil organic carbon is more vulnerable to priming by root exudate fractions than relatively active soil organic carbon. Plant Soil 1–12. https://doi.org/10.1007/s11104-021-05288-y.

Zhou, S., Wang, J., Chen, L., Wang, J., Zhao, F., 2022b. Microbial community structure and functional genes drive soil priming effect following afforestation. Sci. Total Environ. 825, 153925 https://doi.org/10.1016/j.scitotenv.2022.153925.

Zhu, Z., Zhou, J., Shahbaz, M., Tang, H., Liu, S., Zhang, W., Yuan, H., Zhou, P., Alharbi, H., Wu, J., Kuzyakov, Y., Ge, T., 2021. Microorganisms maintain C: N stoichiometric balance by regulating the priming effect in long-term fertilized soils. Appl. Soil Ecol. 167, 104033 https://doi.org/10.1016/j.apsoil.2021.104033.

Zhu, Z., Fang, Y., Liang, Y., Li, Y., Liu, S., Li, Y., Li, B., Gao, W., Yuan, H., Kuzyakov, Y., Wu, J., Richter, A., Ge, T., 2022. Stoichiometric regulation of priming effects and soil carbon balance by microbial life strategies. Soil Biol. Biochem. 108669 https://doi.org/10.1016/j.soilbio.2022.108669.